ACS OMEGA

Article

Cite This: ACS Omega 2018, 3, 18142−18152

http://pubs.acs.org/journal/acsodf

Oxygen by Carbon Replacement at the Glycosidic Linkage Modulates the Sugar Conformation in Tn Antigen Mimics

Claudio D. Navo,*[,†] Iris A. Bermejo,[†] Paula Oroz,[†] Pablo Tovillas,[†] Ismael Compañón,[†] Cristina Matías,[†] Alberto Avenoza,[†] Jesús H. Busto,[†] María M. Zurbano,[†] Gonzalo Jiménez-Osés,[†,‡,§] Francisco Corzana,*[,†] and Jesús M. Peregrina*[,†]

[†]Dept. Química, Centro de Investigación en Síntesis Química, Universidad de La Rioja, E-26006 Logroño, Spain

[‡]CIC bioGUNE, Bizkaia Technology Park, Building 801A, 48170 Derio, Spain

[§]Ikerbasque, Basque Foundation for Science, Maria Diaz de Haro 13, 48009 Bilbao, Spain

Supporting Information

ABSTRACT: *N*-Acetylgalactosamine (GalNAc) α-O-linked to L-threonine (Thr) (Tn antigen) and several mimics of this Tn antigen have been synthesized to explore the impact of the underlying amino acid in the presentation mode of the carbohydrate moiety. The structural changes introduced in the Tn antigen mimics involve the replacement of the natural underlying Thr by non-natural amino acids while maintaining the α-*O*-glycosidic linkage of GalNAc or the substitution of this bond by α-*C*-glycosidic linkages. We also synthesized two bicyclic, conformationally restricted Tn antigen mimics. All of these compounds were subjected to a thorough conformational analysis in solution using NMR data, quantum mechanical (QM) calculations, and molecular dynamics simulations. Interestingly, in *C*-glycosides, the $^1C_4$ chair conformation of the pyranose ring was predicted to be stable by QM calculations and experimentally supported by nuclear Overhauser effect cross-peaks and coupling constants observed in the NMR experiments.

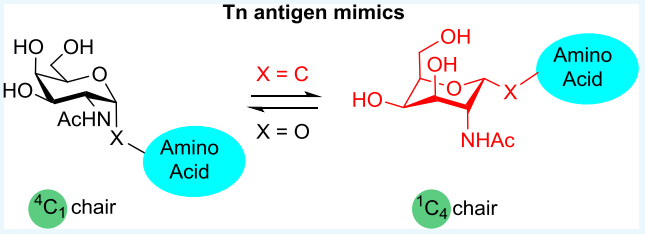

INTRODUCTION

The Tn antigen is a specific human tumor-associated carbohydrate antigen (TACA) formed by *N*-acetylgalactosamine (GalNAc) α-O-linked to either serine (Ser) or threonine (Thr) residues.[1] Although it is quite small and has a simple structure, the Tn antigen has been attracting a great interest because it has been correlated with many types of tumors,[2−13] including breast carcinoma, where it is highly expressed,[2] and it has also been associated to metastatic behavior and tumor expansion.[1,13] In general, the Tn antigen can be found in mucins,[14−16] which are the most abundant glycoproteins in mucus, playing a key role in several biological processes,[17−19] such as tissue inflammation, immune response, or intercellular recognition. In tumor cells, mucins usually present low glycosylation and abnormal sugar chain extensions as a result of the malfunctioning of some glycosyltransferases.[4] This fact results in an exposure of antigens on the surface of cancer cells.[20−23] Consequently, the immune system recognizes these antigens and can trigger an immune response. Different monoclonal antibodies are able to recognize these exposed antigens, binding specifically to cancer cells.

Thus, TACAs and particularly the Tn antigen are considered promising targets for the development of cancer immunotherapy (carbohydrate-based vaccines).[14−16,24−28] Several groups have reported the synthesis and immunological evaluation of cancer therapeutic vaccines, but,[14,29−42] unfortunately, most of the carbohydrate-based vaccines have failed in clinical trials, probably due to immunotolerance or resistance to carbohydrate antibody efficacy.[43] Consequently, there is a great deal of interest in synthesizing non-natural Tn antigen analogues, which would be more resistant to degradation. The synthesis and biological evaluation of analogues of natural carbohydrates and glycopeptides[44−46] can contribute to understanding different biochemical processes and provide new candidates for biological targets. We have reported several examples of non-natural Tn antigen mimics[47−53] comprising minor structural modifications, some of them being able to imitate the conformational preferences of the natural antigens in solution, enhancing the binding affinity to anti-MUC1 antibodies. Herein, we continue exploring this strategy and report new variants in which the underlying amino acid of the Tn antigen (**1**) has been altered and in some cases covalently linked to the carbohydrate to fix the native conformation of the glycosidic linkage.[54−56] The explored modifications include the substitution of Thr by α-methylserine (mimic **2**)[49,52,57] or isoserine (mimic **3**),[52] two compounds already prepared by us but whose conformational analysis has not been accomplished yet. Additionally, we synthesize and analyze in this work novel

Received: September 28, 2018
Accepted: December 4, 2018
Published: December 24, 2018

DOI: 10.1021/acsomega.8b02576
ACS Omega 2018, 3, 18142−18152

Tn antigen mimics (**4**, **5**, and **6**). A cyclic carbamate connecting the *N*-acetyl moiety of GalNAc and the amino group of Thr was introduced in mimic **4**. Other changes include connecting GalNAc to the Cα of Ser, forming a *C*-glycoside derivative (mimic **5**), and incorporating a cyclic urea to generate a bicyclic *C*-glycoside derivative (mimic **6**, Figure 1).

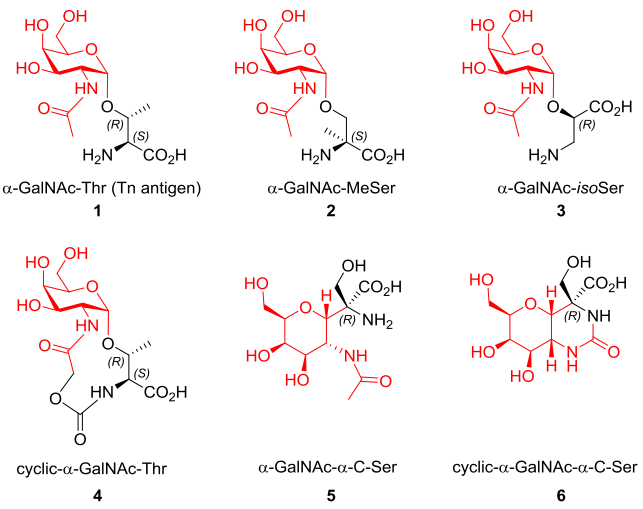

Figure 1. Structures of the natural Tn antigen (**1**) and different non-natural mimics (**2**–**6**) studied in this work.

RESULTS AND DISCUSSION

Synthesis. Initially, we synthesized the Tn antigen mimics **2** and **3** through our recently reported strategy involving the ring-opening of chiral cyclic sulfamidates with carbohydrate C1–*O*-nucleophiles.[52] Thus, starting from effectively accessible (*S*)-α-methylserine and commercially available (*S*)-isoserine, enantiopure cyclic sulfamidates **8** and **9** were efficiently prepared as chiral building blocks for the synthesis of GalNAc-*O*-glycosylated amino acids (*S*)-α-methylserine and (*S*)-isoserine, respectively. The nucleophilic ring-opening reactions of these cyclic sulfamidates **8** and **9** with tri-*O*-acetyl-α-D-*N*-acetylgalactosamine (**7**)[52] using sodium hydride as a base in dimethylformamide were highly chemo-, regio-, and stereoselective and they provided good yields of protected glycosyl-amino-acids **10** and **11**, respectively, which were hydrolyzed to obtain the required Tn antigen mimics **2** and **3** (Scheme 1).

The synthesis of glycoside **4** started with the Koenigs–Knorr glycosylation of *N*-Fmoc-threonine *tert*-butyl ester[58] **13** with tri-*O*-acetyl-protected 2-(azido)galactopyranosyl chloride derivative[59] **12** in the presence of silver salts as promotors, giving a mixture of the α- and β-anomers, which could be purified by column chromatography to obtain α-anomer[60] **14** in a 30% yield (Scheme 2). The azido group of glycoside **14** was transformed into the amino group using Zn in an acidic medium (AcOH and HCl) to obtain compound **15** in a good yield. This compound was treated with bromoacetic acid to generate the corresponding amide **16** using *N*,*N*′-diisopropylcarbodiimide as a coupling reagent and *N*,*N*-diisopropylethylamine as a base in a mixture of tetrahydrofuran (THF)/H_2O at 0 °C for 1 h. The treatment of compound **16** with 1,8-diazabicyclo[5.4.0]undec-7-ene as a non-nucleophilic base in methylene chloride at 0 °C gave the bicyclic compound **17** in a moderate yield. The proposed mechanism involves the abstraction of hydrogen of Fmoc, indicated in blue in Scheme 2, to give 9-methylene-9*H*-fluorene followed by the intramolecular nucleophilic attack of the generated carbamate to the α-bromoacetamide group of the glycosyl moiety. The bromine atom acts as a leaving group to give the corresponding cyclic carbamate **17**. Once purified by column chromatography, the *tert*-butyl ester group was hydrolyzed with trifluoroacetic acid to obtain derivative **18**, which was deacetylated by treatment with sodium methoxide in methanol[61] to give bicyclic glycoside **4** (Scheme 2).

Considering our previous experience in the field of *C*-glycosides,[62,63] we anticipated the synthesis of two *C*-glycosides as new Tn antigen mimics. The starting materials for the synthesis of serine *C*-glycoside **5** were the 2-nitro-tri-*O*-benzyl-D-galactal **19**, obtained following the methodology described by Schmidt and coworkers,[64,65] and the serine-derived *N*,*O*-bicyclic acetals **20a**–**c** synthesized using our

Scheme 1. Synthesis of Tn Antigen Mimics Featuring (*S*)-α-Methylserine (2) or (*S*)-Isoserine (3)[a]

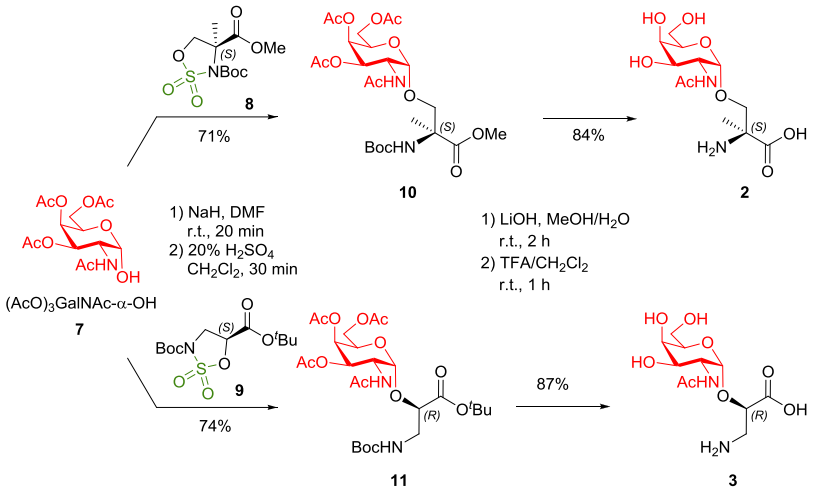

[a]The key step involves the ring-opening reaction of chiral cyclic sulfamidates **8** and **9** with the carbohydrate C1–*O*-nucleophile **7**, followed by hydrolysis of the ring-opened intermediates **10** and **11**.

DOI: 10.1021/acsomega.8b02576
ACS Omega 2018, 3, 18142–18152

Scheme 2. Synthesis of the Tn Antigen Mimic 4

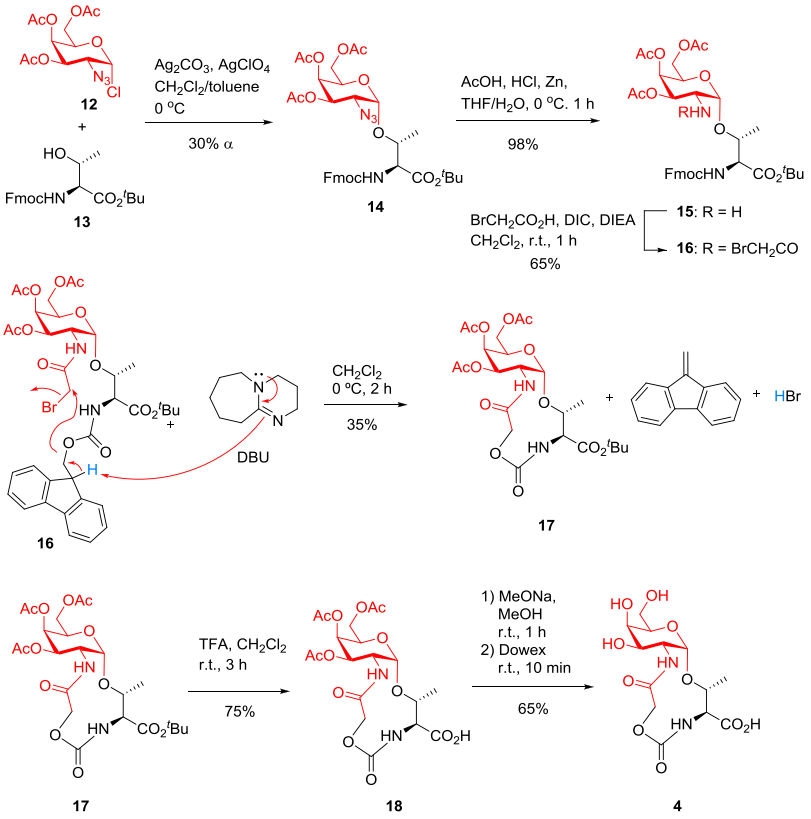

Scheme 3. Synthesis of the Tn Antigen Mimic 5 Using a Michael Addition as a Key Step

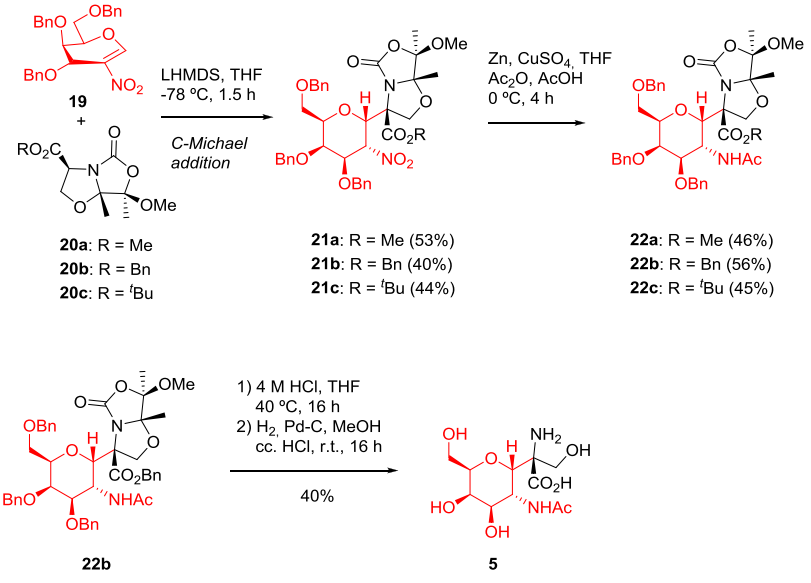

reported methodology[66] from commercially available (*S*)−*N*-Boc-serine methyl ester.

The first step involved a double diastereoselective Michael-type addition of the enolates of bicyclic serine equivalents **20a−c** to the nitrogalactal derivative **19**. THF was used as a solvent, the temperature was set to −78 °C, and lithium bis(trimethylsilyl)amide (LHMDS) was used as a base, obtaining moderate yields of the corresponding Michael adducts **21a−c**, respectively, as previously reported.[62] Notably, in all cases, a unique diastereoisomer **21a**, **21b**, or **21c** was obtained among the eight possible ones. The next step was a selective reduction of the nitro group of compounds **21a−c** and subsequent acetylation of the amines formed. Compounds **21a−c** were treated with Zn and a saturated aqueous solution of $CuSO_4$ in THF−AcOH−Ac_2O (3:2:1) at room temperature for 4 h.[67−69] The corresponding *N*-acetamides **22a−c** were obtained in moderate yields (Scheme 3). Compound **22b** was then reacted with an aqueous 4 M HCl solution in THF at 40 °C for 16 h to afford the corresponding aminoalcohol hydrochloride, which was directly subjected to hydrogenolysis,

DOI: 10.1021/acsomega.8b02576
ACS Omega 2018, 3, 18142−18152

Scheme 4. Synthesis of the Conformationally Restricted Tn Antigen Mimic 6

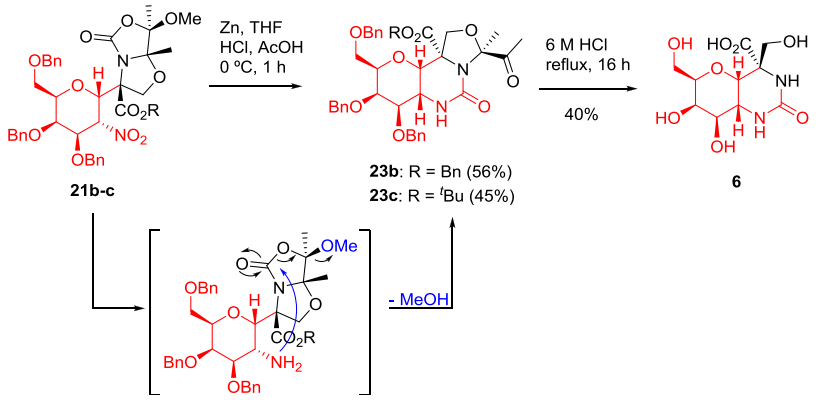

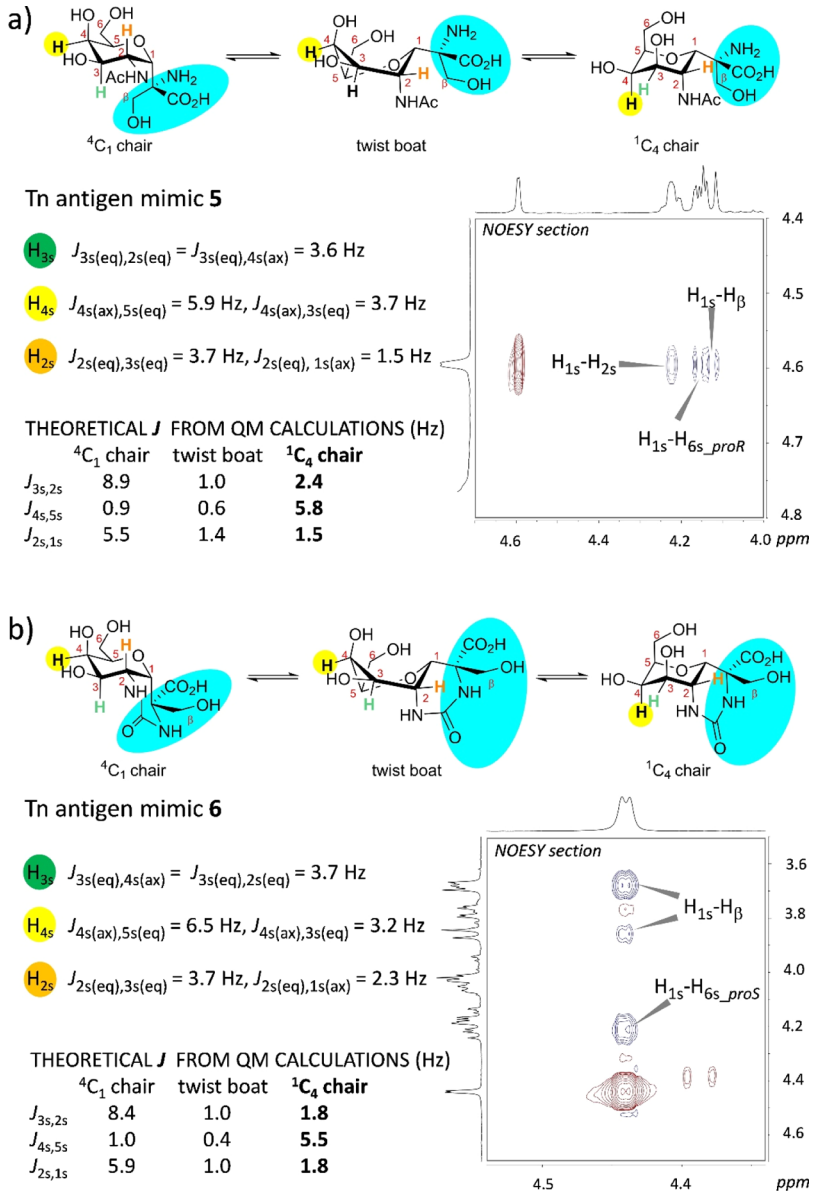

Figure 2. Spatial disposition of H_{3s}, H_{4s}, and H_{2s} protons in $^4C_1$ and $^1C_4$ chair and twist-boat conformations for compounds **5** (a) and **6** (b). According to the coupling constants and the NOESY spectra in H_2O/D_2O (9:1) at 25 °C, in which the most relevant cross-peaks for structural characterization are highlighted, the $^1C_4$ chair conformation should be predominant in solution for compounds **5** and **6**.

using Pd−C as a catalyst in methanol (MeOH) at room temperature for 16 h. Three drops of concentrated HCl were

DOI: 10.1021/acsomega.8b02576
ACS Omega 2018, 3, 18142−18152

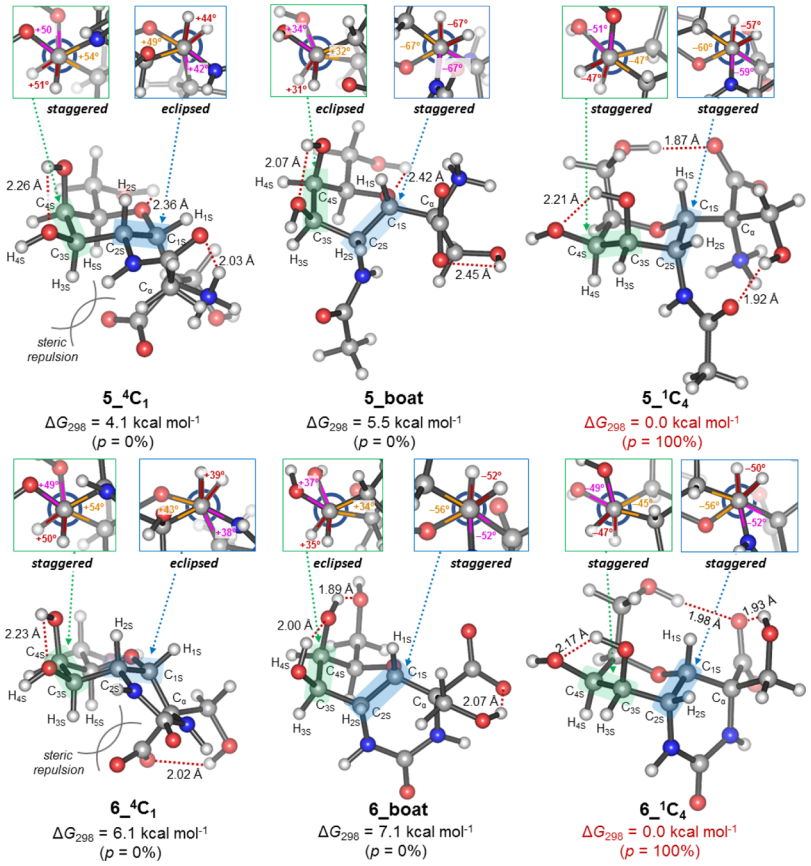

Figure 3. Lowest energy structures for the $^4C_1$ (left), twist-boat (middle), and $^4C_1$ (right) conformations for compounds **5** (top) and **6** (bottom) calculated with PCM(H_2O)/M06-2X/6-31+G(d,p). Free energies at 298 K (ΔG_{298}) are given in kcal mol^{-1} and relative populations (p) derived from ΔG_{298} are shown in parentheses. Torsional strain is represented through the dihedral angles highlighted in three different colors (red, orange, and magenta) at the Newman projections from C 3s to C 4s (carbohydrate, highlighted in green) and from C 2s to C 1s (aglycone, highlighted in blue). Dihedral angles close to ±60° correspond to more staggered conformations. Hydrogen bonds are represented with doted red lines. Distances are given in angstrom.

required to achieve complete deprotection. Purification by reversed-phase high-performance liquid chromatography (RP-HPLC) afforded *C*-glyco-amino-acid **5** (Scheme 3).

The conformationally restricted bicyclic *C*-glycoside **6** was synthesized from Michael adducts **21b** and **21c** (Scheme 4). Treatment of compounds **21b** and **21c** with Zn dust in THF−HCl−AcOH at 0 °C for 1 h reduced their nitro groups into the corresponding amines, which immediately reacted with the oxazolidinone forming bicyclic ureas **23b−c**. Spontaneous carbonyl recovery led to the formation of a pendant methylketone group with concomitant methanol loss. Acidic hydrolysis using an aqueous 6 M HCl solution under reflux for 16 h led to complete deprotection. Purification by RP-HPLC afforded the amino-restricted *C*-glycoside **6** in moderate yield (40%) as a new conformationally restricted Tn antigen mimic (Scheme 4).

Conformational Study. The conformational analysis of the Tn antigen **1** and its mimics (**2−6**) in aqueous solution was then performed by NMR and molecular modeling. While in compounds **1−4** the *α*-*O*-GalNAc unit displays the typical $^4C_1$ chair conformation,[70] in *α*-*C*-glycosides **5** and **6**, the absence of the anomeric effect may promote the coexistence of both $^4C_1$ and $^1C_4$ chairs and the twist-boat.[71−73] In agreement with this notion, the signals of H_{3s} proton observed at 3.86 ppm in the ^{1}H NMR spectrum of compound **5** correspond to a degenerated doublet of doublets that collapses in a pseudo-triplet with two similar small coupling constants of an average value of 3.6 Hz, which is indicative of an equatorial position of this proton and suggesting the prevalence of the $^1C_4$ chair conformation for this compound (Figure 2a). Regarding the small $^3J_{2s,1s}$, with an experimental value of 1.5 Hz, the $^4C_1$ chair conformation can be discarded because in this case, this coupling constant should take values close to 6 Hz. However, with these experimental data, we cannot exclude the occurrence of the twist-boat conformation in solution. Fortunately, although the signals corresponding to H_{4s} and H_{5s} protons are collapsed with other protons, we could extract their coupling constants from the spectra. The value of 5.9 Hz for $^3J_{4s,5s}$ agrees with the existence of the $^1C_4$ chair conformation and is incompatible with both the $^4C_1$ chair and twist-boat conformations. Next, we studied the coupling constants $^3J_{5s,6s\_proS}$ and $^3J_{5s,6s\_proR}$, which give relevant information on the rotamer distribution around the C 5s−C 6s bond. According to their values (2.2 and 10.4 Hz, respectively), we deduced the prevalence of gauche−trans conformation for the hydroxymethyl group. Moreover, with the help of 2D nuclear Overhauser enhancement spectroscopy (NOESY) spectra, H_{6s_proS} and H_{6s_proR} were correctly assigned. Therefore, the medium-size nuclear Overhauser effect (NOE) cross-peaks observed between the anomeric H_{1s} and H_{6s_proR} protons also corroborate the presence of the $^1C_4$ chair in solution (Figure 2a). This NOE is not compatible

DOI: 10.1021/acsomega.8b02576
ACS Omega 2018, 3, 18142−18152

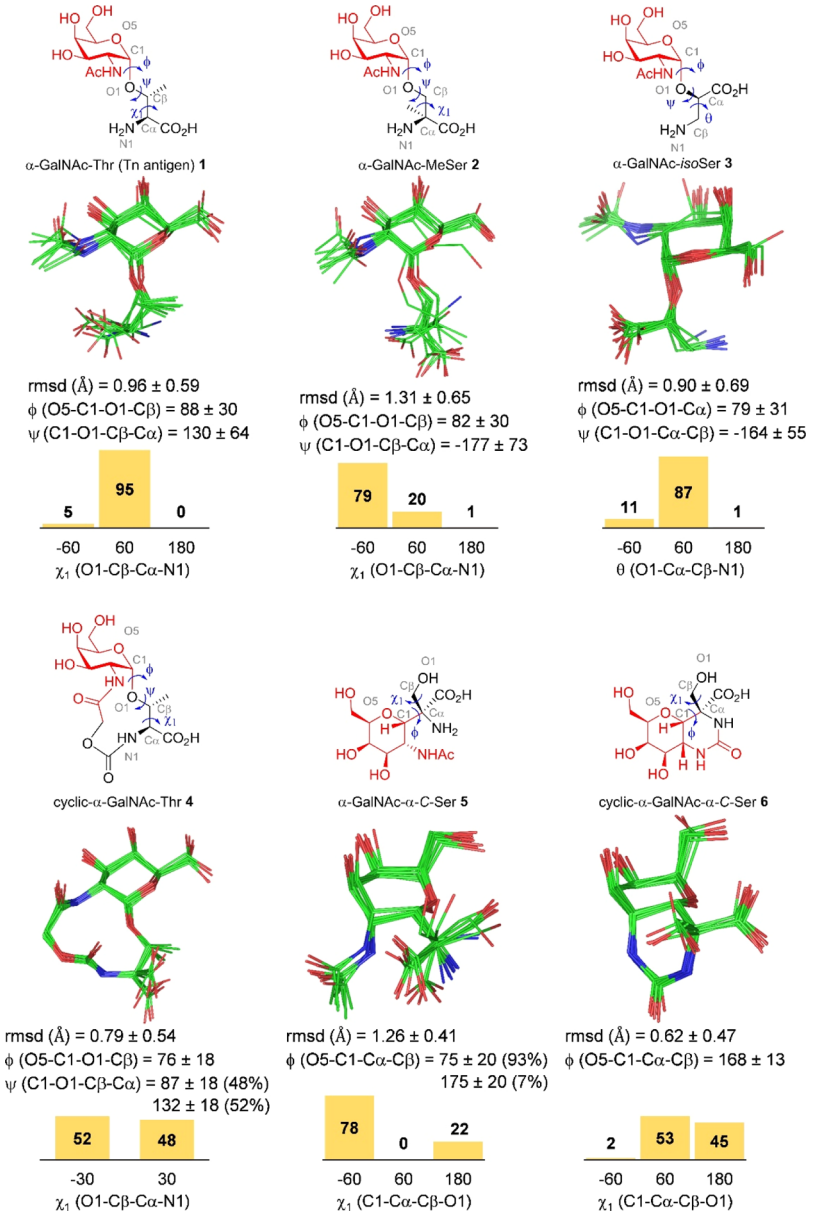

Figure 4. Ensembles derived from the 0.5 μs MD simulations for compound **1** and Tn antigen mimics **2**–**6**. The root-mean-square deviation (Å) values for heavy atom superimposition, together with the main values for the most relevant torsional angles are also indicated. The distribution of χ^1 is shown at the bottom of each derivative.

with the existence of a $^4C_1$ chair or a twist-boat conformer in solution. A similar deduction can be applied to *C*-glycoside **6** (Figure 2b). To conclude the conformational analysis in solution, we accomplished a ^{1}H NMR experiment at different temperatures for compound **6**. Under these conditions, the absence of changes in the signals and in the coupling constant agrees with the existence of a unique conformer in water[74] (Figure S30).

Quantum mechanical (QM) conformational analyses were performed for all compounds, and the lowest energy structures for the $^1C_4$ and $^4C_1$ chair and boat conformations in compounds **5** and **6** were calculated with PCM(H_2O)/M06-2X/6-31+G(d,p). In line with the experimental NMR data, the free energies obtained indicated that the $^1C_4$ chair conformation is the most stable arrangement for the carbohydrate moiety of Tn antigen mimics **5** and **6** (Figure 3 and Supporting Information). In the same way, in the case of the hydroxymethyl group conformation of the saccharide fragment, the gauche−trans arrangement shows prevalence over the trans−gauche or gauche−gauche dispositions in all studied compounds. These data are in agreement with previous published works.[75,76] Exceptionally, in bicyclic system **6**, we observed that the gauche−gauche is isoenergetic with gauche−trans disposition. Additionally, to corroborate our conformational deductions from the NMR data, we calculated the key coupling constants (Figure 2, see *J* values in bold) using the dihedral angles obtained from the optimized geometries for the lowest energy conformers and the Karplus-like equations implemented in the MestReJ software,[77] matching very well with the $^1C_4$ chair conformation.

It is well known that the $^4C_1$ chair conformation is the most stable for *O*-glycosides with a pyranose structure and is determined mainly by the anomeric and exo-anomeric effects.[71−73] This fact occurs in Tn mimics **1**–**4** as we can

DOI: 10.1021/acsomega.8b02576
ACS Omega 2018, 3, 18142−18152

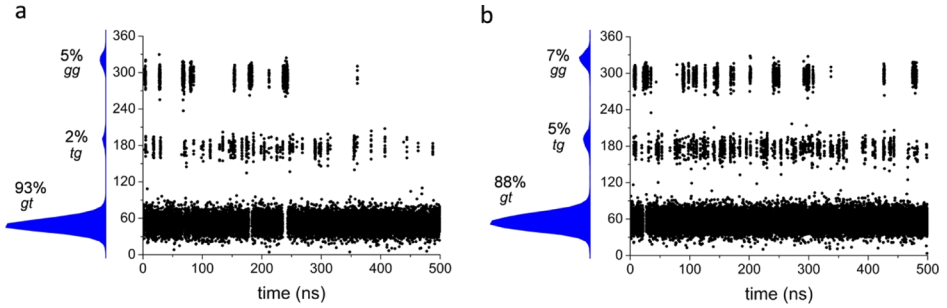

Figure 5. Rotamer distribution around the C 5s−C 6s bond derived from 0.5 μs MD simulations for Tn mimics **5** (a) and **6** (b). The values of the torsional angle ω (O5−C5−C6−O6) are shown.

see in the structures obtained from molecular dynamics (MD) simulations (see below, Figure 4). However, these electronic effects do not exist when the oxygen is replaced by a carbon atom at the glycosidic linkage in derivatives **5** and **6** (*C*-glycosides).

The greater stability of the $^1C_4$ chair conformations in both α-*C*-glycosides **5** and **6** with respect to the $^4C_1$ chair and twist-boat conformations can be attributed to a number of additive contributions. First, the lack of anomeric effects due to the absence of α-*O*-glycosidic bonds at the anomeric carbon C 1s precludes the normal stabilization of the $^4C_1$ chair because of donor−acceptor interactions from the O 5s endocyclic oxygen lone pairs (n_{Oendo}) to the antibonding orbital of the C 1s−OR bond ($\sigma^*_{C1-Oexo}$) (endo-anomeric effect) and from the OR exocyclic oxygen lone pairs (n_{Oexo}) to the antibonding orbital of the C 1s−O 5s bond ($\sigma^*_{C1-Oendo}$) (exo-anomeric effect).[71−73] Second, accumulation of torsional strain at the carbohydrate moiety in the twist-boats and at the aglycone region in the $^4C_1$ chairs (Figure 3, see highlighted dihedral angles) destabilizes these arrangements with respect to the $^1C_4$ conformations, which avoid such torsional strain by placing substituents at C 1s and C 2s in relaxed equatorial and axial dispositions, respectively. On the contrary, the presence of bulky carboxylate groups at Cα of the aglycone distorts the C 1s−Cα bond from axial to pseudoaxial disposition in the $^4C_1$ chairs,[78] thus increasing torsional strain, particularly in the bicyclic compound **6**. As a result, this compound adopts a much more stable *cis*-decalin-like arrangement which overcomes the 1,3-diaxial strain arising from placing the C 3s−hydroxy and C 5s−hydroxymethyl groups in mutually axial positions. Finally, the aglycone Cα−carboxylate groups establish strong hydrogen bond networks in the $^1C_4$ chair conformations of both compounds **5** and **6**, which contribute to largely stabilize this unusual arrangement with respect to the $^4C_1$ chair and twist-boat conformations.

Next, 0.5 μs MD simulations in explicit water were performed on compounds **1**−**6**. The most stable $^1C_4$ chair conformation was used in the starting structures of compounds **5** and **6**. The conformational ensembles obtained for derivatives are shown in Figure 4, and the normalized frequencies of the most relevant dihedral angles for compounds **1**−**6** are depicted in Figure S31. The good agreement between the experimental and theoretical $J_{H\alpha,H\beta}$ coupling constants obtained for compound **1** (2.0 and 2.4 Hz, respectively) validate the MD simulations on this natural derivative.[54−56] Additionally, average $^3J_{H,H}$ values extracted from this MD simulations for compounds **5** and **6** are in agreement with experimental $^3J_{H-H}$ values extracted from NMR experiments in D_2O and with theoretical $^3J_{H-H}$ values for the quantum mechanics-calculated minimum energy structures of the $^1C_4$ conformations (Tables S1 and S2). According to the MD simulations, the ϕ torsional angle displays values close to 80° in compounds **1**−**4**, in good accordance with the exo-anomeric effect.[71−73] While in compound **1**, the glycosidic linkage shows the typical "eclipsed" conformation, in derivatives **2** and **3**, the staggered conformation is mainly populated. As previously reported by us,[57] the glycosidic linkage of compound **2** was flexible when the underlying amino acid was presented as a diamide. However, the zwitterion form favors a rigid side chain, with a main value for (χ^1) close to −60°. In compound **4**, although the global structure is rigid, two similarly populated conformers were found for both ψ and χ^1 torsional angles. On the other hand and in good agreement with the QM calculations commented above, **5** and **6** display a rigid *C*-glycosidic linkage. We also analyzed the conformational preferences of the hydroxymethyl group of the sugar moiety. In compounds **1** and **2**, featuring a $^4C_1$ chair conformation, a mixture of the gauche−trans (60%) and trans−gauche (26%) is observed, as deduced experimentally from the values of $^3J_{5s,6s\_proS}$ and $^3J_{5s,6s\_proR}$ (4.7 and 7.5 Hz, respectively). This result agrees with previous studies performed on galactose derivatives.[79] On the contrary, in Tn mimics **5** and **6**, which display the $^1C_4$ chair disposition, the gauche−trans rotamer is mainly populated (87%). This experimental outcome is reproduced by the MD simulations (Figure 5) and agrees with the experimental values of the coupling constants (Tables S1 and S2).

Our MD simulations indicate that the intramolecular hydrogen bonds for compounds **1**−**6** are irrelevant for their 3D disposition, with populations in all cases <20%. This result agrees with the radial distribution functions calculated for all derivatives (Figure S32).[80] Finally, to delimit the role of water in the conformational preferences of these derivatives, we performed the analysis of the first hydration shell. Interestingly, NH_3^+ promotes the existence of bridging water molecules between the carbohydrate and amino acid moieties not only in the Tn bearing a threonine residue (Tn−Thr)[55] but also in derivatives **2** and **3** (Figure 6). This feature can contribute to rigidify these derivatives in water. A similar localized water density is found between the NH groups of derivative **4**, mimicking the conformational behavior of the Tn−Thr antigen.

Altogether, these data indicate that mimics **1**−**6** are rather stiff, displaying a main conformation in solution.

CONCLUSIONS

Several mimics of the Tn antigen have been synthesized by replacing the natural underlying threonine by the non-natural

DOI: 10.1021/acsomega.8b02576
ACS Omega 2018, 3, 18142−18152

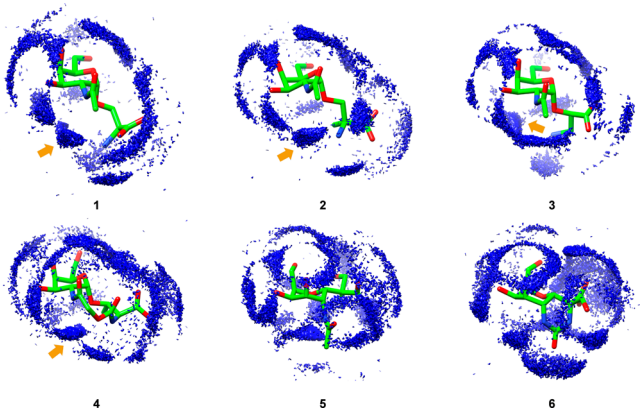

Figure 6. Averaged first hydration shell derived from 0.5 μs MD simulations for compounds **1**−**5**. The arrows show the localized water pockets found in compounds **1**−**4** between the amino acid and carbohydrate moieties.

amino acids isoserine and α-methylserine, either maintaining the α-*O*-glycosidic linkage with the GalNAc moiety or replacing this bond by α-*C*-glycosidic linkages. Additionally, on the basis of our preliminary conformational studies on the Tn antigen,[54−56] in which we demonstrated the rigidity of the glycosidic bond and the water-mediated connection between the carbohydrate and amino acid moieties, we synthesized two bicyclic Tn antigen mimics. The conformational analysis using NMR, QM, and MD of all of the studied compounds suggests that in *C*-glycoside derivatives, the pyranose ring adopts a $^1C_4$ chair conformation. In future works, we will evaluate the binding affinity of these Tn mimics toward different targets of biological interest.

EXPERIMENTAL SECTION

Reagent and General Procedures. We have included in the Supporting Information a section to describe thoroughly the commercial reagents used, the synthetic protocols followed, and the apparatus used to characterize the compounds. Moreover, the synthesis of all compounds is described in the Supporting Information.

NMR Experiments. NMR protocols and equipment used to carry out the NMR experiments (^{1}H and ^{13}C NMR, COSY, HSQC, and NOESY) are detailed in the Supporting Information.

MD Simulations. The calculations were performed using the AMBER 16 package[81] implemented with GAFF2[82] force field. More details are shown in the Supporting Information.

Quantum Mechanics. Full geometry optimizations were performed using Gaussian 16[83] with the M06-2X hybrid functional[84] and 6-31+G(d,p) basis set. Bulk solvent effects in water were considered implicitly using the IEF-PCM polarizable continuum model.[85] Different conformations were considered for all structures. More information is detailed in the Supporting Information.

ASSOCIATED CONTENT

Supporting Information

The Supporting Information is available free of charge on the ACS Publications website at DOI: 10.1021/acsomega.8b02576.

Additional experimental details, NMR spectra, and computational information including figures (PDF)

AUTHOR INFORMATION

Corresponding Authors

*E-mail: claudio-daniel.navon@unirioja.es (C.D.N.).
*E-mail: francisco.corzana@unirioja.es (F.C.).
*E-mail: jesusmanuel.peregrina@unirioja.es (J.M.P.).

ORCID

Gonzalo Jiménez-Osés: 0000-0003-0105-4337
Francisco Corzana: 0000-0001-5597-8127
Jesús M. Peregrina: 0000-0003-3778-7065

Notes

The authors declare no competing financial interest.

ACKNOWLEDGMENTS

We are grateful to MINECO (projects CTQ2015-67727-R and UNLR13-4E-1931 to J.M.P. and F.C., CTQ2015-70524-R and RYC-2013-14706 to G.J.-O. and C.D.N.). I.A.B. thanks the Asociación Española Contra el Cáncer en La Rioja (AECC) for a grant. We also thank CESGA (Universidad de Santiago de Compostela) and BERONIA (Universidad de La Rioja) for computer support. F.C. thanks the EU (Marie-Sklodowska Curie ITN, ProteinConjugates).

REFERENCES

(1) Ju, T.; Otto, V. I.; Cummings, R. D. The Tn antigen-structural simplicity and biological complexity. *Angew. Chem., Int. Ed.* **2011**, *50*, 1770−1791.
(2) Springer, G. F.; Desai, P. R.; Banatwala, I. Blood group MN specific substances and precursors in normal and malignant human breast tissues. *Naturwissenschaften* **1974**, *61*, 457−458.
(3) Davidson, B.; Berner, A.; Nesland, J. M.; Risberg, B.; Kristensen, G. B.; Tropé, C. G.; Bryne, M. Carbohydrate antigen expression in primary tumors, metastatic lesions, and serous effusions from patients diagnosed with epithelial ovarian carcinoma: Evidence of up-regulated Tn and Sialyl Tn antigen expression in effusions. *Hum. Pathol.* **2000**, *31*, 1081−1087.
(4) Costa, C.; Pereira, S.; Lima, L.; Peixoto, A.; Fernandes, E.; Neves, D.; Neves, M.; Gaiteiro, C.; Tavares, A.; da Costa, R. M. G.; Cruz, R.; Amaro, T.; Oliveira, P. A.; Ferreira, J. A.; Santos, L. L. Abnormal protein glycosylation and activated PI3K/Akt/mTOR pathway: Role in bladder cancer prognosis and targeted therapeutics. *PLoS One* **2015**, *10*, e0141253.
(5) Hirao, T.; Sakamoto, Y.; Kamada, M.; Hamada, S.-I.; Aono, T. Tn antigen, a marker of potential for metastasis of uterine cervix cancer cells. *Cancer* **1993**, *72*, 154−159.
(6) Terasawa, K.; Furumoto, H.; Kamada, M.; Aono, T. Expression of Tn and Sialyl-Tn antigens in the neoplastic transformation of uterine cervical epithelial cells. *Cancer Res* **1996**, *56*, 2229−32.
(7) Itzkowitz, S. H.; Yuan, M.; Montgomery, C. K.; Kjeldsen, T.; Takahashi, H. K.; Bigbee, W. L.; Kim, Y. S. Expression of Tn, sialosyl-Tn, and T antigens in human colon cancer. *Cancer Res* **1989**, *49*, 197−204.
(8) Byrd, J. C.; Bresalier, R. S. Mucins and mucin binding proteins in colorectal cancer. *Cancer Metastasis Rev.* **2004**, *23*, 77−99.
(9) López-Ferrer, A.; Barranco, C.; de Bolós, C. Differences in the O-glycosylation patterns between lung squamous cell carcinoma and adenocarcinoma. *Am. J. Clin. Pathol.* **2002**, *118*, 749−755.
(10) Ohshio, G.; Imamura, T.; Imamura, M.; Yamabe, H.; Sakahara, H.; Nakada, H.; Yamashina, I. Distribution of Tn antigen recognized by an anti-Tn monoclonal antibody (MLS128) in normal and malignant tissues of the digestive tract. *J. Cancer Res. Clin. Oncol.* **1995**, *121*, 247−252.
(11) Remmers, N.; Anderson, J. M.; Linde, E. M.; DiMaio, D. J.; Lazenby, A. J.; Wandall, H. H.; Mandel, U.; Clausen, H.; Yu, F.; Hollingsworth, M. A. Aberrant expression of mucin core proteins and

DOI: 10.1021/acsomega.8b02576
ACS Omega 2018, 3, 18142−18152

O-linked glycans associated with progression of pancreatic cancer. *Clin. Cancer Res.* **2013**, *19*, 1981−1993.
(12) Zhang, S.; Zhang, H. S.; Reuter, V. E.; Slovin, S. F.; Scher, H. I.; Livingston, P. O. Expression of potential target antigens for immunotherapy on primary and metastatic prostate cancers. *Clin Cancer Res* **1998**, *4*, 295−302.
(13) Fu, C.; Zhao, H.; Wang, Y.; Cai, H.; Xiao, Y.; Zeng, Y.; Chen, H. Tumor-associated antigens: Tn antigen, sTn antigen, and T antigen. *HLA* **2016**, *88*, 275−286.
(14) Strous, G. J.; Dekker, J. Mucin-type glycoproteins. *Crit. Rev. Biochem. Mol. Biol.* **1992**, *27*, 57−92.
(15) Hang, H. C.; Bertozzi, C. R. The chemistry and biology of mucin-type O-linked glycosylation. *Bioorg. Med. Chem.* **2005**, *13*, 5021−5034.
(16) Fumoto, M.; Hinou, H.; Ohta, T.; Ito, T.; Yamada, K.; Takimoto, A.; Kondo, H.; Shimizu, H.; Inazu, T.; Nakahara, Y.; Nishimura, S.-I. Combinatorial synthesis of MUC1 glycopeptides: Polymer blotting facilitates chemical and enzymatic synthesis of highly complicated mucin glycopeptides. *J. Am. Chem. Soc.* **2005**, *127*, 11804−11818.
(17) Dwek, R. A. Glycobiology: Toward understanding the function of sugars. *Chem. Rev.* **1996**, *96*, 683−720.
(18) Sears, P.; Wong, C.-H. Enzyme action in glycoprotein synthesis. *Cell. Mol. Life Sci.* **1998**, *54*, 223−252.
(19) Johansson, M. E. V.; Hansson, G. C. Immunological aspects of intestinal mucus and mucins. *Nat. Rev. Immunol.* **2016**, *16*, 639−649.
(20) Sell, S. Cancer-associated carbohydrates identified by monoclonal antibodies. *Hum. Pathol.* **1990**, *21*, 1003−1019.
(21) Hakomori, S.-I.; Zhang, Y. Glycosphingolipid antigens and cancer therapy. *Chem. Biol.* **1997**, *4*, 97−104.
(22) Taylor-Papadimitriou, J.; Epenetos, A. A. Exploiting altered glycosylation patterns in cancer: Progress and challenges in diagnosis and therapy. *Trends Biotechnol.* **1994**, *12*, 227−233.
(23) Gabius, H.-J. Animal lectins. *Eur. J. Biochem.* **1997**, *243*, 543−576.
(24) Buskas, T.; Thompson, P.; Boons, G.-J. Immunotherapy for cancer: synthetic carbohydrate-based vaccines. *Chem. Commun.* **2009**, 5335−5349.
(25) Gaidzik, N.; Westerlind, U.; Kunz, H. The development of synthetic antitumour vaccines from mucin glycopeptide antigens. *Chem. Soc. Rev.* **2013**, *42*, 4421−4442.
(26) Wolfert, M. A.; Boons, G.-J. Adaptive immune activation: glycosylation does matter. *Nat. Chem. Biol.* **2013**, *9*, 776−784.
(27) Wilson, R. M.; Danishefsky, S. J. A vision for vaccines built from fully synthetic tumor-associated antigens: From the laboratory to the clinic. *J. Am. Chem. Soc.* **2013**, *135*, 14462−14472.
(28) Cai, H.; Sun, Z.-Y.; Chen, M.-S.; Zhao, Y.-F.; Kunz, H.; Li, Y.-M. Synthetic multivalent glycopeptide-lipopeptide antitumor vaccines: impact of the cluster effect on the killing of tumor cells. *Angew. Chem., Int. Ed.* **2014**, *53*, 1699−1703.
(29) Keil, S.; Claus, C.; Dippold, W.; Kunz, H. Towards the development of antitumor vaccines: A Synthetic Conjugate of a Tumor-Associated MUC1 Glycopeptide Antigen and a Tetanus Toxin Epitope. *Angew. Chem., Int. Ed.* **2001**, *40*, 366−369.
(30) Brocke, C.; Kunz, H. Synthesis of tumor-associated glycopeptide antigens. *Bioorg. Med. Chem.* **2002**, *10*, 3085−3112.
(31) Dziadek, S.; Kunz, H. Synthesis of tumor-associated glycopeptide antigens for the development of tumor-selective vaccines. *Chem. Rec.* **2004**, *3*, 308−321.
(32) Lai, Z.; Schreiber, J. R. Antigen processing of glycoconjugate vaccines; the polysaccharide portion of the pneumococcal CRM(197) conjugate vaccine co-localizes with MHC II on the antigen processing cell surface. *Vaccine* **2009**, *27*, 3137−3144.
(33) Costantino, P.; Rappuoli, R.; Berti, F. The design of semi-synthetic and synthetic glycoconjugate vaccines. *Expert Opin. Drug Discovery* **2011**, *6*, 1045−1066.
(34) Tarp, M. A.; Clausen, H. Mucin-type O-glycosylation and its potential use in drug and vaccine development. *Biochim. Biophys. Acta, Gen. Subj.* **2008**, *1780*, 546−563.
(35) Hanisch, F.-G.; Ninkovic, T. Immunology of O-glycosylated proteins: approaches to the design of a MUC1 glycopeptide-based tumor vaccine. *Curr. Protein Pept. Sci.* **2006**, *7*, 307−315.
(36) Martínez-Sáez, N.; Peregrina, J. M.; Corzana, F. Principles of mucin structure: implications for the rational design of cancer vaccines derived from MUC1-glycopeptides. *Chem. Soc. Rev.* **2017**, *46*, 7154−7175.
(37) Danishefsky, S. J.; Allen, J. R. From the laboratory to the clinic: A retrospective on fully synthetic carbohydrate-based anticancer vaccines. *Angew. Chem., Int. Ed.* **2000**, *39*, 836−863.
(38) Slovin, S. F.; Ragupathi, G.; Musselli, C.; Olkiewicz, K.; Verbel, D.; Kuduk, S. D.; Schwarz, J. B.; Sames, D.; Danishefsky, S.; Livingston, P. O.; Scher, H. I. Fully synthetic carbohydrate-based vaccines in biochemically relapsed prostate cancer: Clinical trial results with α-N-acetylgalactosamine-O-serine/threonine conjugate vaccine. *J. Clin. Oncol.* **2003**, *21*, 4292−4298.
(39) Galonić, D. P.; Gin, D. Y. Chemical glycosylation in the synthesis of glycoconjugate antitumour vaccines. *Nature* **2007**, *446*, 1000−1007.
(40) Dube, D. H.; Bertozzi, C. R. Glycans in cancer and inflammation - potential for therapeutics and diagnostics. *Nat. Rev. Drug Discovery* **2005**, *4*, 477−488.
(41) Ragupathi, G.; Coltart, D. M.; Williams, L. J.; Koide, F.; Kagan, E.; Allen, J.; Harris, C.; Glunz, P. W.; Livingston, P. O.; Danishefsky, S. J. On the power of chemical synthesis: immunological evaluation of models for multiantigenic carbohydrate-based cancer vaccines. *Proc. Natl. Acad. Sci. U.S.A.* **2002**, *99*, 13699−13704.
(42) Buskas, T.; Ingale, S.; Boons, G.-J. Towards a fully synthetic carbohydrate-based anticancer vaccine: synthesis and immunological evaluation of a lipidated glycopeptide containing the tumor-associated Tn antigen. *Angew. Chem., Int. Ed.* **2005**, *44*, 5985−5988.
(43) Beatty, G. L.; Gladney, W. L. Immune escape mechanisms as a guide for cancer immunotherapy. *Clin. Cancer Res.* **2014**, *21*, 687−692.
(44) Westerlind, U. Synthetic glycopeptides and glycoproteins with applications in biological research. *Beilstein J. Org. Chem.* **2012**, *8*, 804−818.
(45) Jiménez-Barbero, J.; Dragoni, E.; Venturi, C.; Nannucci, F.; Ardá, A.; Fontanella, M.; André, S.; Cañada, F. J.; Gabius, H.-J.; Nativi, C. Alpha-O-linked glycopeptide mimetics: synthesis, conformation analysis and interactions with viscumin, a galactoside-binding model lectin. *Chem.—Eur. J.* **2009**, *15*, 10423−10431.
(46) Koester, D. C.; Holkenbrink, A.; Werz, D. B. Recent advances in the synthesis of carbohydrate mimetics. *Synthesis* **2010**, 3217−3242.
(47) Martínez-Sáez, N.; Castro-López, J.; Valero-González, J.; Madariaga, D.; Compañón, I.; Somovilla, V. J.; Salvadó, M.; Asensio, J. L.; Jiménez-Barbero, J.; Avenoza, A.; Busto, J. H.; Bernardes, G. J. L.; Peregrina, J. M.; Hurtado-Guerrero, R.; Corzana, F. Deciphering the non-equivalence of serine and threonine O-glycosylation points: Implications for molecular recognition of the Tn antigen by an anti-MUC1 antibody. *Angew. Chem., Int. Ed.* **2015**, *54*, 9830−9834.
(48) Rojas-Ocáriz, V.; Compañón, I.; Aydillo, C.; Castro-Lopez, J.; Jiménez-Barbero, J.; Hurtado-Guerrero, R.; Avenoza, A.; Zurbano, M. M.; Peregrina, J. M.; Busto, J. H.; Corzana, F. Design of α-S-neoglycopeptides derived from MUC1 with a flexible and solvent-exposed sugar moiety. *J. Org. Chem.* **2016**, *81*, 5929−5941.
(49) Martínez-Sáez, N.; Supekar, N. T.; Wolfert, M. A.; Bermejo, I. A.; Hurtado-Guerrero, R.; Asensio, J. L.; Jiménez-Barbero, J.; Busto, J. H.; Avenoza, A.; Boons, G.-J.; Peregrina, J. M.; Corzana, F. Mucin architecture behind the immune response: Design, evaluation and conformational analysis of an antitumor vaccine derived from an unnatural MUC1 fragment. *Chem. Sci.* **2016**, *7*, 2294−2301.
(50) Somovilla, V. J.; Bermejo, I. A.; Albuquerque, I. S.; Martínez-Sáez, N.; Castro-López, J.; García-Martín, F.; Compañón, I.; Hinou, H.; Nishimura, S.-I.; Jiménez-Barbero, J.; Asensio, J. L.; Avenoza, A.; Busto, J. H.; Hurtado-Guerrero, R.; Peregrina, J. M.; Bernardes, G. J. L.; Corzana, F. The use of fluoroproline in MUC1 antigen enables

DOI: 10.1021/acsomega.8b02576
ACS Omega 2018, 3, 18142−18152

efficient detection of antibodies in patients with prostate cancer. *J. Am. Chem. Soc.* **2017**, *139*, 18255−18261.
(51) Fernández, E. M. S.; Navo, C. D.; Martínez-Sáez, N.; Gonçalves-Pereira, R.; Somovilla, V. J.; Avenoza, A.; Busto, J. H.; Bernardes, G. J. L.; Jiménez-Osés, G.; Corzana, F.; Fernández, J. M. G.; Mellet, C. O.; Peregrina, J. M. Tn antigen mimics based on sp2-iminosugars with affinity for an anti-MUC1 antibody. *Org. Lett.* **2016**, *18*, 3890−3893.
(52) Tovillas, P.; García, I.; Oroz, P.; Mazo, N.; Avenoza, A.; Corzana, F.; Jiménez-Osés, G.; Busto, J. H.; Peregrina, J. M. Tn antigen mimics by ring-opening of chiral cyclic sulfamidates with carbohydrate C1-S- and C1-O-nucleophiles. *J. Org. Chem.* **2018**, *83*, 4973−4980.
(53) Aydillo, C.; Compañón, I.; Avenoza, A.; Busto, J. H.; Corzana, F.; Peregrina, J. M.; Zurbano, M. M. S-Michael additions to chiral dehydroalanines as an entry to glycosylated cysteines and a sulfa-Tn antigen mimic. *J. Am. Chem. Soc.* **2014**, *136*, 789−800.
(54) Corzana, F.; Busto, J. H.; Jiménez-Osés, G.; Asensio, J. L.; Jiménez-Barbero, J.; Peregrina, J. M.; Avenoza, A. New insights into α-GalNAc−Ser motif: Influence of hydrogen bonding versus solvent interactions on the preferred conformation. *J. Am. Chem. Soc.* **2006**, *128*, 14640−14648.
(55) Corzana, F.; Busto, J. H.; Jiménez-Osés, G.; de Luis, M. G.; Asensio, J. L.; Jiménez-Barbero, J.; Peregrina, J. M.; Avenoza, A. Serine versus threonine glycosylation: The methyl group causes a drastic alteration on the carbohydrate orientation and on the surrounding water shell. *J. Am. Chem. Soc.* **2007**, *129*, 9458−9467.
(56) Bermejo, I. A.; Usabiaga, I.; Compañón, I.; Castro-López, J.; Insausti, A.; Fernández, J. A.; Avenoza, A.; Busto, J. H.; Jiménez-Barbero, J.; Asensio, J. L.; Peregrina, J. M.; Jiménez-Oses, G.; Hurtado-Guerrero, R.; Cocinero, E. J.; Corzana, F. Water sculpts the distinctive shapes and dynamics of the Tn antigens: Implications for their molecular recognition. *J. Am. Chem. Soc.* **2018**, *140*, 9652.
(57) Corzana, F.; Busto, J. H.; Marcelo, F.; de Luis, M. G.; Asensio, J. L.; Martín-Santamaría, S.; Sáenz, Y.; Torres, C.; Jiménez-Barbero, J.; Avenoza, A.; Peregrina, J. M. Rational design of a Tn antigen mimic. *Chem. Commun.* **2011**, *47*, 5319−5321.
(58) Paulsen, H.; Adermann, K. Synthesis of O-glycopeptides of the N-terminus of interleukin-2. *Liebigs Ann. Chem.* **1989**, *1989*, 751−769.
(59) Plattner, C.; Höfener, M.; Sewald, N. One-pot azido-chlorination of glycals. *Org. Lett.* **2011**, *13*, 545−547.
(60) Koeller, K. M.; Smith, M. E. B.; Wong, C.-H. Chemoenzymatic synthesis of PSGL-1 glycopeptides: Sulfation on tyrosine affects glycosyltransferase-catalyzed synthesis of the O-glycan. *Bioorg. Med. Chem.* **2000**, *8*, 1017−1025.
(61) Zerong, W. *Comprehensive Organic Name Reactions and Reagents*; John, Wiley & Sons, Inc., 2010; pp 3123−3128.
(62) Aydillo, C.; Navo, C. D.; Busto, J. H.; Corzana, F.; Zurbano, M. M.; Avenoza, A.; Peregrina, J. M. A double diastereoselective Michael-type addition as an entry to conformationally restricted Tn antigen mimics. *J. Org. Chem.* **2013**, *78*, 10968−10977.
(63) Navo, C. D.; Corzana, F.; Sánchez-Fernández, E. M.; Busto, J. H.; Avenoza, A.; Zurbano, M. M.; Nanba, E.; Higaki, K.; Mellet, C. O.; Fernández, J. M. G.; Peregrina, J. M. Conformationally-locked C-glycosides: tuning aglycone interactions for optimal chaperone behaviour in Gaucher fibroblasts. *Org. Biomol. Chem.* **2016**, *14*, 1473−1484.
(64) Winterfeld, G. A.; Ito, Y.; Ogawa, T.; Schmidt, R. R. A Novel and efficient route towards α-GalNAc-Ser and α-GalNAc-Thr building blocks for glycopeptide synthesis. *Eur. J. Org. Chem.* **1999**, 1167−1171.
(65) Winterfeld, G. A.; Schmidt, R. R. Nitroglycal concatenation: A broadly applicable and efficient approach to the synthesis of complex O-glycans. *Angew. Chem., Int. Ed.* **2001**, *40*, 2654−2657.
(66) Aydillo, C.; Jiménez-Osés, G.; Busto, J. H.; Peregrina, J. M.; Zurbano, M. M.; Avenoza, A. Theoretical evidence for pyramidalized bicyclic serine enolates in highly diastereoselective alkylations. *Chem.—Eur. J.* **2007**, *13*, 4840−4848.
(67) Lee, D. J.; Harris, P. W. R.; Brimble, M. A. Synthesis of MUC1 neoglycopeptides using efficient microwave-enhanced chaotrope-assisted click chemistry. *Org. Biomol. Chem.* **2011**, *9*, 1621−1626.
(68) Meinjohanns, E.; Meldal, M.; Schleyer, A.; Paulsen, H.; Bock, K. Efficient syntheses of core 1, core 2, and core 3 and core 4 building blocks for SPS of mucin O-glycopeptides based on the N-Dts-method. *J. Chem. Soc., Perkin Trans. 1* **1996**, 985−993.
(69) Bourgault, J. P.; Trabbic, K. R.; Shi, M.; Andreana, P. R. Synthesis of the tumor associative α-aminooxy disaccharide of the TF antigen and its conjugation to a polysaccharide immune stimulant. *Org. Biomol. Chem.* **2014**, *12*, 1699−1702.
(70) Mayes, H. B.; Broadbelt, L. J.; Beckham, G. T. How sugars pucker: Electronic structure calculations map the kinetic landscape of five biologically paramount monosaccharides and their implications for enzymatic catalysis. *J. Am. Chem. Soc.* **2014**, *136*, 1008−1022.
(71) Asensio, J. L.; Cañada, F. J.; García-Herrero, A.; Murillo, M. T.; Fernández-Mayoralas, A.; Johns, B. A.; Kozak, J.; Zhu, Z.; Johnson, C. R.; Jiménez-Barbero, J. Conformational Behavior of Aza-C-Glycosides: Experimental Demonstration of the Relative Role of the exo-anomeric Effect and 1,3-Type Interactions in Controlling the Conformation of Regular Glycosides. *J. Am. Chem. Soc.* **1999**, *121*, 11318−11329.
(72) Asensio, J. L.; Cañada, F. J.; Cheng, X.; Khan, N.; Mootoo, D. R.; Jiménez-Barbero, J. Conformational Differences Between O- and C-Glycosides: The α-O-Man-(1−>1)-β-Gal/α-C-Man-(1−−>1)-β-Gal Case − A Decisive Demonstration of the Importance of the exo-Anomeric Effect on the Conformation of Glycosides. *Chem.—Eur. J.* **2000**, *6*, 1035−1041.
(73) Wiberg, K. B.; Bailey, W. F.; Lambert, K. M.; Stempel, Z. D. The anomeric effect: It's complicated. *J. Org. Chem.* **2018**, *83*, 5242−5255.
(74) Unione, L.; Xu, B.; Díaz, D.; Martín-Santamaría, S.; Poveda, A.; Sardinha, J.; Rauter, A. P.; Blériot, Y.; Zhang, Y.; Cañada, F. J.; Sollogoub, M.; Jiménez-Barbero, J. Conformational Plasticity in Glycomimetics: Fluorocarbamethyl-L-idopyranosides Mimic the Intrinsic Dynamic Behaviour of Natural Idose Rings. *Chem.—Eur. J.* **2015**, *21*, 10513−10521.
(75) Stenutz, R.; Carmichael, I.; Widmalm, G.; Serianni, A. S. Hydroxymethyl group conformation in saccharides: structural dependencies of $^{2}J_{HH}$, $^{3}J_{HH}$, and $^{1}J_{CH}$ spin-spin coupling constants. *J. Org. Chem.* **2002**, *67*, 949−958.
(76) Thibaudeau, C.; Stenutz, R.; Hertz, B.; Klepach, T.; Zhao, S.; Wu, Q.; Carmichael, I.; Serianni, A. S. Correlated C−C and C−O Bond Conformations in Saccharide Hydroxymethyl Groups: Parametrization and Application of Redundant $^{1}H-^{1}H$, $^{13}C-^{1}H$, and $^{13}C-^{13}C$ NMR J-Couplings. *J. Am. Chem. Soc.* **2004**, *126*, 15668−15685.
(77) Navarro-Vázquez, A.; Cobas, J. C.; Sardina, F. J.; Casanueva, J.; Díez, E. A Graphical Tool for the Prediction of Vicinal Proton-Proton $^{3}J_{HH}$ Coupling Constants. *J. Chem. Inf. Comput. Sci.* **2004**, *44*, 1680−1685.
(78) Leclerc, E.; Pannecoucke, X.; Ethève-Quelquejeu, M.; Sollogoub, M. Fluoro-C-glycosides and fluoro-carbasugars, hydrolytically stable and synthetically challenging glycomimetics. *Chem. Soc. Rev.* **2013**, *42*, 4270−4283.
(79) Kirschner, K. N.; Woods, R. J. Solvent interactions determine carbohydrate conformation. *Proc. Natl. Acad. Sci. U.S.A.* **2001**, *98*, 10541−10545.
(80) Soper, A. K. The radial distribution functions of water and ice from 220 to 673 K and at pressures up to 400 MPa. *Chem. Phys.* **2000**, *258*, 121−137.
(81) Case, D. A.; Betz, R. M.; Cerutti, D. S.; Cheatham, T. E., III; Darden, T. A.; Duke, R. E.; Giese, T. J.; Gohlke, H.; Goetz, A. W.; Homeyer, N.; Izadi, S.; Janowski, P.; Kaus, J.; Kovalenko, A.; Lee, T. S.; LeGrand, S.; Li, P.; Lin, C.; Luchko, T.; Luo, R.; Madej, B.; Mermelstein, D.; Merz, K. M.; Monard, G.; Nguyen, H.; Nguyen, H. T.; Omelyan, I.; Onufriev, A.; Roe, D. R.; Roitberg, A.; Sagui, C.; Simmerling, C. L.; Botello-Smith, W. M.; Swails, J.; Walker, R. C.;

DOI: 10.1021/acsomega.8b02576
ACS Omega 2018, 3, 18142−18152

Wang, J.; Wolf, R. M.; Wu, X.; Xiao, L.; Kollman, P. A. *AMBER 2016*; University of California: San Francisco, 2016.
(82) Wang, J.; Wolf, R. M.; Caldwell, J. W.; Kollman, P. A.; Case, D. A. Development and testing of a general amber force field. *J. Comput. Chem.* **2004**, *25*, 1157−1174.
(83) Frisch, M. J.; Trucks, G. W.; Schlegel, H. B.; Scuseria, G. E.; Robb, M. A.; Cheeseman, J. R.; Scalmani, G.; Barone, V.; Petersson, G. A.; Nakatsuji, H.; Li, X.; Caricato, M.; Marenich, A. V.; Bloino, J.; Janesko, B. G.; Gomperts, R.; Mennucci, B.; Hratchian, H. P.; Ortiz, J. V.; Izmaylov, A. F.; Sonnenberg, J. L.; Williams-Young, D.; Ding, F.; Lipparini, F.; Egidi, F.; Goings, J.; Peng, B.; Petrone, A.; Henderson, T.; Ranasinghe, D.; Zakrzewski, V. G.; Gao, J.; Rega, N.; Zheng, G.; Liang, W.; Hada, M.; Ehara, M.; Toyota, K.; Fukuda, R.; Hasegawa, J.; Ishida, M.; Nakajima, T.; Honda, Y.; Kitao, O.; Nakai, H.; Vreven, T.; Throssell, K.; Montgomery, J. A., Jr.; Peralta, J. E.; Ogliaro, F.; Bearpark, M. J.; Heyd, J. J.; Brothers, E. N.; Kudin, K. N.; Staroverov, V. N.; Keith, T. A.; Kobayashi, R.; Normand, J.; Raghavachari, K.; Rendell, A. P.; Burant, J. C.; Iyengar, S. S.; Tomasi, J.; Cossi, M.; Millam, J. M.; Klene, M.; Adamo, C.; Cammi, R.; Ochterski, J. W.; Martin, R. L.; Morokuma, K.; Farkas, O.; Foresman, J. B.; Fox, D. J. *Gaussian 09*; Gaussian, Inc.: Wallingford CT, 2016.
(84) Zhao, Y.; Truhlar, D. G. The M06 suite of density functionals for main group thermochemistry, thermochemical kinetics, noncovalent interactions, excited states, and transition elements: two new functionals and systematic testing of four M06-class functionals and 12 other functionals. *Theor. Chem. Acc.* **2007**, *120*, 215−241.
(85) Scalmani, G.; Frisch, M. J. Continuous surface charge polarizable continuum models of solvation. I. General formalism. *J. Chem. Phys.* **2010**, *132*, 114110.

DOI: 10.1021/acsomega.8b02576
ACS Omega 2018, 3, 18142−18152